Proceedings of the Korean Nuclear Society Autumn Meeting
Seoul, Korea, October 1995

Numerical Prediction of Turbulent Flow in Bare Rod Bundles Using Control Volume Based Finite Element Method

In Young Im and Jong Sik Cheong
Korea Atomic Energy Research Institute

Abstract

Turbulent flow field in a subchannel of bare rod bundles has been numerically simulated using the control volume based finite element method. Launder & Ying model of Reynolds stress and Lam & Bremhorst low-Reynolds number model are implemented in k-ε equations and momentum equations. Secondary flows are simulated using the stream function and vorticity approach. The control volume based finite element method enable to use the upwind scheme (donor cell scheme). Sensitivity of the constants in the models are studied, and proper values are found to get the close result to the measured flow distributions.

1. Introduction

Thermal hydraulic parameters such as pressure drop coefficient and heat transfer coefficient of turbulent flow have been determined usually using the empirical correlations. However, more accurate prediction of thermal hydraulic parameters or flow field is required for special geometries or flow conditions. Especially, prediction of flow field in rod bundle has been required for the safety analysis of nuclear reactor. Cross flow due to turbulence between the subchannels is one parameter for the determination of thermal margin of nuclear reactor core.

There have been disputes on the turbulence induced crossflow mechanism whether the mean flow distribution can be predicted with secondary flow simulation with isotropic properties, or only with anisotropy adjustment. Seale[1] insisted that the secondary flow effect did not play major role in mean velocity distortions, and that using the anisotropy affective diffusivity, distortions in mean velocity distribution were predicted. However, Rapley and Gosman[2] simulated the turbulent flow structure numerically, and showed that with secondary flow, predictions of mean flow and turbulence kinetic energy distributions were fairly close to the experimental results. Rapley and Gosman used general orthogonal curvilinear mesh based numerical finite volume method and they implied that they had difficulties in obtaining the converged solutions.

Patankar[3] noted that direct application of pure Galerkin weighted residual method gave almost the same troubles as when the central difference scheme in finite difference method was used. To avoid the troubles such as wavy pressures, Baliga and Patankar[4] developed control volume based finite element method (CVFEM). They applied CVFEM to the convection diffusion problems and fluid flow problems. For the fluid flow problems, they applied SIMPLER algorithm with CVFEM[5].

In this study, the basic idea of CVFEM is used for the prediction of flow field in rod bundle array. Mapping according to the flow direction[4,5] has not been used. Only upwind scheme (donor cell scheme)[6] is applied. Also, using the stream function and vorticity equations, pure diffusion and convection equations are solved.

Numerical simulations are performed for triangular subchannel with various pitch(P) to diameter(D) ratios (P/D). The results show the same trend as in the results of previous works[2,12]. Sensitivity study was made for the constants in Launder and Ying model and low Reynolds number model. Optimal values of constants are selected to get the results close to the measured values.

2. Control Volume based FEM

Two dimensional convection-diffusion equation with source term is expressed as ;

$$\frac{\partial \phi}{\partial t}+\frac{\partial u\phi}{\partial x}+\frac{\partial v\phi}{\partial y}-\frac{\partial}{\partial x}(\Gamma\frac{\partial \phi}{\partial x})-\frac{\partial}{\partial y}(\Gamma\frac{\partial \phi}{\partial y}) = S(x,y). \tag{1}$$

Instead of setting up the set of difference equations in x-y coordinate with given $\triangle$x, $\triangle$y, one can obtain a set of linear equations by integrating this equation over each control volumes. Area integration can be converted into line integration using the Green-Gauss theorem.

$$\int_{\Omega}\left[\frac{\partial u\phi}{\partial x}+\frac{\partial v\phi}{\partial y}-\frac{\partial}{\partial x}(\Gamma\frac{\partial \phi}{\partial x})-\frac{\partial}{\partial y}(\Gamma\frac{\partial \phi}{\partial y})\right] d\Omega$$

$$= \int_{c}(u\phi+v\phi)ds-\int_{c}\Gamma(\frac{\partial \phi}{\partial x}+\frac{\partial \phi}{\partial y})ds \tag{2}$$

where s is the boundary line of each control volume and the integration is in counterclock wise. The first term in right hand side is net convection rate across the segment of control volume boundary line. According to the flow direction, ϕ value is determined. For triangular element, control volume is setup as in Figure 1.

$$Q = \int udy-vdx \tag{3}$$

For segment a-r-o, when the sign of Q is positive, ϕ is given of ϕ_P and when the sign of Q is negative, ϕ is given ϕ_K. This is the application of upwind scheme in finite element method. Linear interpolation functions are used for each element using nodal values. And finally, a set of discretization equations are obtained.

$$\sum a_{nb}\phi_p = \sum a_{nb}\phi_{nb}+d_p \tag{4}$$

$$\text{where} \quad d_p = \int S\, d\Omega = \sum_{i=1}^{k} A_iS_i/3 \tag{5}$$

and k is the number of elements adjacent to node P, nb is neighbor nodes around P, and A_i is the area of element i.

3. Turbulent Flow in Subchannels

Turbulent flow in subchannels are numerically simulated using momentum equations and continuity equation. The Reynolds stress are modeled using the

Launder & Ying model[7]. This model is expressed using the variables of k and ε, the turbulence kinetic energy and turbulence energy dissipation rate, respectively. The k-ε model is expressed as

$$\frac{\partial \rho k}{\partial t} + \frac{\partial \rho U_j k}{\partial x_j} = \left(\frac{\mu_t}{\sigma_k}\nabla^2 k + g - \rho\varepsilon\right) \tag{6}$$

$$\frac{\partial \rho \varepsilon}{\partial t} + \frac{\partial \rho U_j \varepsilon}{\partial x_j} = \left(\frac{\mu_t}{\sigma_\varepsilon}\nabla^2 \varepsilon + C_{\varepsilon 1} g \frac{\varepsilon}{k} - C_{\varepsilon 2}\rho\frac{\varepsilon^2}{k}\right) \tag{7}$$

$$\text{where } g \equiv \mu_t \left(\frac{\partial U_i}{\partial x_j}\left(\frac{\partial U_i}{\partial x_j} + \frac{\partial U_j}{\partial x_i}\right)\right) \tag{8}$$

$$k \equiv \frac{1}{2}\overline{\rho u_i u_i},\ C_{\varepsilon 1}=1.44,\ C_{\varepsilon 2}=1.92,\ \sigma_k=1.0,\ \sigma_\varepsilon=1.3. \tag{9}$$

Using the Launder & Ying model and setting

$$\nu_t \equiv C_4 \frac{k_2}{\varepsilon},\quad C_4 = 0.085, \tag{10}$$

we have an expression of axial momentum equation as

$$\frac{\partial W}{\partial t} + \frac{\partial UW}{\partial x} + \frac{\partial VW}{\partial y} = (\nu+\nu_t)\nabla^2 W - \frac{1}{\rho}\frac{\partial P}{\partial z} \tag{11}$$

Secondary flow momentum equations are converted into stream function and vorticity equations.

- Vorticity equation

$$\rho\frac{\partial \omega}{\partial t} + \rho U\frac{\partial \omega}{\partial x} + \rho V\frac{\partial \omega}{\partial y} = \mu\nabla^2\omega + \rho\frac{\partial^2}{\partial x \partial y}(\overline{u^2}-\overline{v^2}) - \rho\left(\frac{\partial^2 \overline{uv}}{\partial x^2} - \frac{\partial^2 \overline{uv}}{\partial y^2}\right) \tag{12}$$

From Launder & Ying model,

$$\overline{u^2}-\overline{v^2} = -C_2 C_4 \left(\frac{k^3}{\varepsilon^2}\right)\left[\left(\frac{\partial W}{\partial x}\right)^2-\left(\frac{\partial W}{\partial y}\right)^2\right] \tag{13}$$

$$\overline{uv} = -C_2 C_4 \left(\frac{k^3}{\varepsilon^2}\right)\left(\frac{\partial W}{\partial x}\right)\left(\frac{\partial W}{\partial y}\right)$$

Vorticity (ω) is defined as

$$\omega \equiv \frac{\partial V}{\partial x} - \frac{\partial U}{\partial y} \tag{14}$$

and by the definition of stream function,

$$\frac{\partial \psi}{\partial y} = \rho U, \qquad \frac{\partial \psi}{\partial x} = -\rho V \tag{15}$$

stream function equation is obtained.

$$\nabla^2 \psi = -\rho\omega \tag{16}$$

Boundary conditions for the k-ε equations at near wall are defined by Lam & Bremhorst low-Reynolds number model[8]. This model modifies constants of equations (7) and (10). Using following definition

$$R_k \equiv \sqrt{k}L/\nu,\quad R_t \equiv k^2/\nu\varepsilon \tag{17}$$

(L is the distance from the wall.) one can calculate the multipliers ;

$$f_\mu = (1-e^{-A_\mu R_k})^2(1+\frac{20.5}{R_t}), \quad A_\mu = 0.0165$$
$$f_1 = 1+(\frac{0.05}{f_\mu})^3, \quad f_2 = 1-e^{-R_t^2} \tag{18}$$

And following modifications are suggested

$$\nu_t = C_4 f_\mu \frac{k^2}{\varepsilon} \tag{19}$$

$$\frac{\partial \rho\varepsilon}{\partial t} + \frac{\partial \rho U_j \varepsilon}{\partial x_j} = (\frac{\mu_t}{\sigma_\varepsilon}\nabla^2\varepsilon + C_{\varepsilon 1} f_1 g \frac{\varepsilon}{k} - C_{\varepsilon 2} f_2 \rho \frac{\varepsilon^2}{k}). \tag{20}$$

With these modification, k values at the wall are set to be zero, and normal gradient of ε at the wall can be set to be zero. This low-Reynolds number is required when the y+ value at the first node from the wall is not sufficiently greater than 11.5.

4. Numerical Simulation

Typical model of finite elements has been used as shown in Figure 2. This model is mapped according to the pitch to diameter ratio, and subchannel type (triangular or square). 656 triangular elements with 367 nodes (maximum node number = 391) are used. Under-relaxation and small time steps are used for the stability of iterative calculation. Following boundary conditions are used. For axial mean velocity, zero for the wall nodes and normal gradients are zero at the symmetry boundaries. For stream function, all the boundary values are zero. Normal gradients of vorticity at the symmetry boundaries are zero, and at the wall nodes following relations are used [9].

$$\omega_w = -[\frac{3(\psi_P - \psi_w)}{\rho h^2} + \frac{\omega_P}{2}] \tag{21}$$

where subscript P represents the value of the adjacent node and h is the distance between these two nodes. Turbulence kinetic energy, k, at the wall node is zero, and normal gradients at the symmetry boundaries are zero. All the normal gradients of ε at the boundaries are zero[8]. Axial flow momentum equation, k- ε equations, and vorticity equation are all the standard convection diffusion equations, and direct application of CVFEM is possible. The stream function equation is pure diffusion equation.

Since these equations are strongly coupled each other, careful iteration is required. First assuming the ν_t distribution, axial mean flow distribution is calculated. Turbulence production term, g in equation (8), is calculated from mean flow distribution and k- ε equations are solved. The k- ε equations are strongly coupled each other and highly nonlinear, very small time step and under-relaxation are required. During the iteration ν_t is updated. With the k and ε distribution, the source terms of vorticity equation are calculated according to the Launder & Ying model for the turbulence fluctuation term. Calculated vorticity distribution is used for the source terms of stream function equation. Since the stream function and vorticity equations are coupled each other in boundary condition, inner iteration is required. From the stream function distribution, secondary flow velocities are calculated by definition of the stream

function, and these secondary flow velocities are used for the other equations.

Triangular subchannels are analyzed for two cases with different pitch to diameter ratio (P/D). First case is the experiment of Carajilescov and Todreas[10]. In this case, P/D ratio is 1.123 and Reynolds number is 27000. For this case, Carajilescov and Todreas performed analytical prediction also. Later, Rapley[2] simulated this case numerically with general orthogonal curvilinear mesh based numerical finite volume method, and obtained better result with single swirl of secondary flow.

First, effects of the constant C_2 in Launder & Ying model on the axial mean flow distribution are investigated. Increase of the constant C_2 from 0.013 (Rapley used this value) makes $\xi(W/W_{avg})$ at point A smaller, i.e., makes mean velocity distribution flat at the inner region. Thus, the difference between the measured and predicted values at point B decreases. However, the difference at point A increases. The turbulence kinetic energy distribution shows good agreement with Rapley's prediction, but still predictions are higher than the measured values. Also, it can be noted that the turbulence kinetic energy decreases with increase of C_2.

Effects of the constant in low-Reynolds number model has been investigated. Equation (17) has empirically determined constant, A_μ. This constant determines the steepness of the multiplying factor at near wall nodes. When we used A_μ, 0.0140 instead of 0.0165, we obtained k distribution shown in Figure 3, which shows very good agreement with the measured data. Also, it modifies mean velocity distribution. When we use higher A_μ than 0.0165, the ξ value at point A increases. With the informations from these numerical tests, Figure 4 is obtained which shows the mean flow distribution with selected C_2 and A_μ. The differences between the predicted and the measured are very small.

Second case is for the Trupp and Azad experiment[11]. They measured mean flow velocities for various Reynolds number conditions at P/D=1.2. Figure 5 shows the comparison between the predicted and measured mean velocity contours. With carefully selected constants of C_2 and A_μ, the good agreement with the measured data is achieved.

Figure 6 shows typical stream functions for P/D of 1.123 and 1.2. Single swirl has been predicted by Rapley and Lee[12], for P/D=1.123. Also, no distortions are found for the stream functions for the case of P/D=1.2. For this case, Rapley's prediction has distortion around point B.

5. Conclusion

Control volume based Finite Element Method has been applied for the simulation of turbulent flow in subchannel of bare rod bundle array. This numerical scheme gives good convergency and good results. Sensitivity of the constants in Launder & Ying model and in Lam & Bremhorst low-Reynolds number model has been studied, and optimal constants were selected. With carefully selected constants, prediction results show much better agreement to the measurements than the previous works.

References ;

1. W.J. Seale, "Turbulent Diffusion of Heat Between Connected Flow Passages," Nuclear Engineering and Design 54(1979) 197-209.
2. C.W. Rapley and A.D. Gosman, "The Prediction of Fully Developed Axial Turbulent Flow in Rod Bundles," Nuclear Engineering and Design 97(1986) 313-325.
3. S.V. Patankar, Numerical Heat Transfer and Fluid Flow, Hemisphere, Washington, D.C., 1980.
4. B.R. Baliga and S.V. Patankar, "A New Finite-Element Formulation for Convection-Diffusion Problems," Numerical Heat Transfer, vol.3, pp.393-409, 1980.
5. N.A. Hookey and B.R. Baliga, "Evaluation and Enhancement of Some Control Volume Finite-Element Methods - Part 2. Incompressible Fluid Flow Problems," Numerical Heat Transfer, vol.14, pp.273-293, 1988.
6. G.E. Schneider and M.J. Raw, "A Skewed, Positive Influence Coefficient Upwinding Procedure for Control-Volume-Based Finite-Element Convection-Diffusion Computation," Numerical Heat Transfer, vol.9, pp.1-26, 1986.
7. B.E. Launder and W.M. Ying, "Prediction of Flow and Heat Transfer in Ducts of Square Cross Section," Proceedings of the Institution of Mechanical Engineers, vol.187, 1973.
8. C.G.K. Lam and K. Bremhorst, "A Modified Form of the k-ε Model for Predicting Wall Turbulence," ASME J. Fluids Engineering, vol.103, pp.456-460, 1981.
9. T.J. Chung, Finite Element Analysis in Fluid Dynamics, McGraw-Hill, Inc., 1978.
10. P. Carajilescov and N.E. Todreas, "Experimental and Analytical Study of Axial Turbulent Flows in an Interior Subchannel of a Bare Rod Bundle," ASME J. Heat Transfer, vol.98, pp.262-268, 1976.
11. A.C. Trupp and R.S. Azad, "The Structure of Turbulent Flow in Triangular Array Rod Bundles," Nuclear Engineering and Design, vol.32, pp.47-84, 1975.
12. K.B. Lee, H.C. Jang and S.K. Lee, "Study of the Secondary Flow Effect on the Turbulent Flow Characteristics in Fuel Rod Bundles," J. of KNS, vol.26, pp.345-354, 1994.

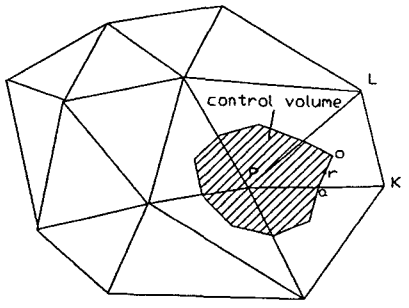

Figure 1. Definitions of Control Volume and Upwind Scheme

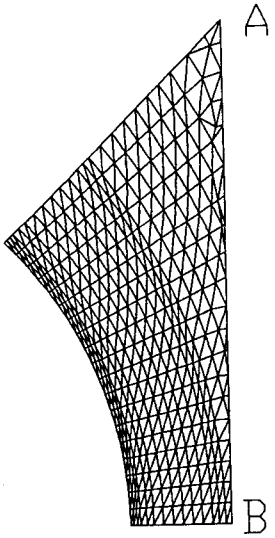

Figure 2. Typical Nodalization of the Subchannel and Location of Points A and B

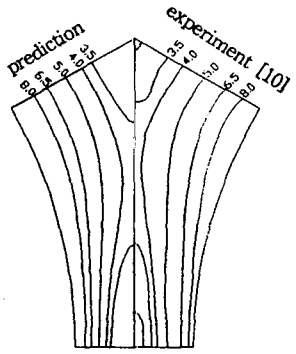

Figure 3. Turbulence Kinetic Energy ($k*10^3/W_{avg}^2$) Distribution at Triangular Subchannel
P/D=1.123, Re=27000, C_2=0.013, A_μ= 0.014

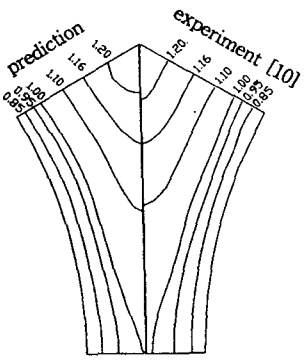

Figure 4. Mean Velocity Distribution (W/W_{avg}) at Triangular Subchannel
P/D=1.123, Re=27000,
C_2=0.013*3.0, A_μ= 0.0165*1.25

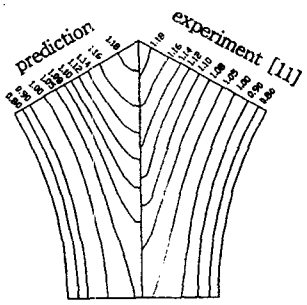

a : Re=26000, C_2= 0.013*2.5

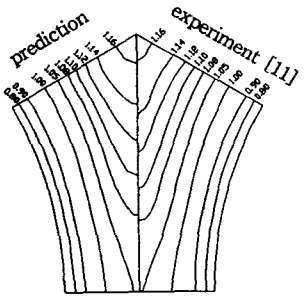

b : Re=56070, C_2= 0.013*3.0

Figure 5. Mean Velocity Distribution (W/W_{avg}) at Triangular Subchannel
P/D=1.2, A_μ=0.0165*1.25

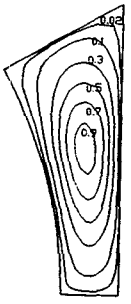

a : P/D=1.123, Re=27000

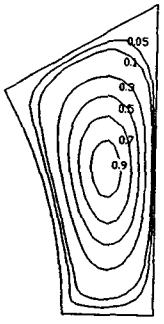

b : P/D=1.2, Re=56070

Figure 6. Stream Lines(ψ/ψ_{max}) for the Secondary Flow in Triangular Subchannel
C_2=0.013*3.0, A_μ=0.0165*1.25